Structure and stability of the interface between graphene and 6H-SiC(000-1) (3x3) : an STM and ab-initio study

Fanny Hiebel, Laurence Magaud, Pierre Mallet, Jean-Yves Veuillen

Structure and stability of the interface between graphene and 6H-SiC(000-1) (3x3) : an STM and ab-initio study.

F Hiebel, L Magaud, P Mallet and J-Y Veuillen*

Institut Néel, CNRS-UJF, Boîte Postale 166, 38042 Grenoble, France

* Corresponding author

E-mails : fanny.hiebel@grenoble.cnrs.fr, laurence.magaud@grenoble.cnrs.fr, pierre.mallet@grenoble.cnrs.fr, jean-yves.veuillen@grenoble.cnrs.fr

Abstract

We examine in detail the structure and the evolution upon annealing of the SiC(3x3) reconstruction which is known to be present at the interface between the SiC-C face substrate and the graphene layer for samples prepared in high vacuum. We use ab-initio calculations to test the validity of proposed or classical structural models in comparison with scanning tunnelling microscopy (STM) images. We analyze the electronic structure of the bare surface and detect interface states which can pin the surface Fermi level. From a comparison of the signal coming from the bare and graphene covered SiC(3x3) reconstruction we propose that the transparency of the graphene in high bias STM images results from an enhancement of the local density of states of the interface plane by the graphene layer. We discuss the thermal stability of the SiC(3x3) surface, and show that it transforms more easily into the $SiC(2x2)_C$ reconstruction in the graphene covered region than for the bare surface. This evolution generates both structural and electronic heterogeneities at the interface.

PACS numbers : 73.20._r, 73.22.Pr, 81.05.ue, 68.37.Ef, 68.65.Pq, 71.15.Mb

Introduction

From the beginning of the investigations of the physical properties of graphene [1, 2], sample preparation by controlled sublimation of hexagonal (polar) SiC surfaces has been shown to be a viable route for preparing high quality layers [3, 4]. The as-grown graphene layers are in contact with the underlying substrate through an interface layer, which consists of a chemically modified or reconstructed substrate surface. Two different substrate faces are commonly used for graphene growth: the 6H(4H)-SiC(0001), also called the Si face, and the 6H(4H)-SiC(000-1), called the C face. In either case, it can be anticipated that the structure of the interface layer will determine some important physical properties of the neighbouring graphene layer, for instance the native carrier concentration (via charge transfer from the interface [5, 6]) or the electron scattering through charged interface

defects [7, 8]. More importantly, it is known that the band structure of the first graphitic layer can be severely distorted by interaction with the substrate, resulting in the removal of the characteristic “Dirac cones” at the K/K’ points [9, 10, 11, 12]. It is thus important to have a detailed description of the interface for a proper understanding of the material properties.

Graphene grows on SiC as a result of preferential Si sublimation [13]. Different procedures have been used for sample preparation. Sublimation in ultra-high vacuum (UHV) provides samples with well defined interfaces, at the expense of small domain sizes [14]. Grain sizes can be largely increased by controlling the Si sublimation rate, either by working in an inert gaz atmosphere [15, 16], by providing an external Si flux [17] or by using a confined geometry [18, 19]. Especially the high structural quality of graphene layers prepared by the confinement controlled sublimation (CCS) process [19] has been confirmed by many experiments (for a review see [20]).

For the samples prepared on the Si face, the structure of the interface seems to be independent of the fabrication process for the as-grown samples [15, 17, 19, 21]. The interface can be chemically modified by post-growth processes [22, 23, 24], which results in some improvement of the transport properties [25]. The situation is different for the C face, since the interface exhibits either genuine SiC reconstructions (for the samples prepared under UHV [12, 26, 27, 28]) or a simple SiC(1x1) low energy electron diffraction (LEED) pattern (for samples made using the CCS technique [29]). The UHV prepared samples have an inhomogeneous interface since two different SiC surface reconstructions are simultaneously present in general [27, 28]. Although the samples prepared using the CCS process do not show any apparent reconstruction of the SiC surface in LEED, Mathieu et al [29] have revealed some heterogeneity at the interface by means of spectro-microscopy. The results suggest the existence of two different bonding configurations between the substrate and the graphene layer, which are reflected in the amount of charge transfer [29]. The origin of these configurations is not clear yet, although different possibilities have been suggested [29]. It is thus worth exploring the different sources of heterogeneity at the interface in graphene layers prepared on the C face of SiC. In this paper, we address this issue by means of scanning tunnelling microscopy (STM) combined with ab-initio calculations. Although the study is performed only on UHV grown samples, we believe that it can give valuable clues in order to understand the interface structure in samples from different origin.

The paper is organized as follows. In the first section we summarize the investigation techniques we have used, including the sample preparation procedure. Section 2 is devoted to the detailed investigation of the structure of one of the SiC surface reconstructions, the SiC(3x3), which is known to be present at the interface. The SiC(3x3) is studied here for the bare surface in order to get information on the surface gap states. Section 3 is devoted to the investigation of the graphene-SiC(3x3) interface. A detailed account of this system has already been given [30]. Hence, in a first part, we only summarize the main results and give additional information on the doping level. In a second part, we present a semi-quantitative investigation of the ubiquitous “transparency” of graphene

in high bias STM images. Finally, in section 4, we analyze the thermal stability of the SiC(3x3) interface reconstruction, pointing to a preferential evolution towards the $SiC(2x2)_C$ structure in graphene covered areas.

1. Technical details

1.1. Sample preparation and characterization

The samples have been prepared under ultra high vacuum (UHV) conditions following the recipe given in Ref. [27, 30]. After sample outgazing, the 6H-SiC(000-1) surface is cleaned at 850°C under an Si flux. Subsequent annealing without Si flux at 950-1000°C leads to the 6H-SiC(000-1) (3x3) surface reconstruction [31], denoted SiC(3x3) in the following. This surface is lightly graphitized by further annealing at higher temperature (15 minutes annealing for each step) until a graphitic signal is detected by low energy electron diffraction (LEED). As reported in previous studies of UHV grown samples [12, 13, 26, 27, 28] the diffraction pattern of graphene on the C face appears as a circle with modulated intensities. This indicates a rotational disorder in the orientation of the graphene islands on the surface, although preferential orientations exist. At that stage the substrate still presents a dominant (3x3) reconstruction from LEED, but usually faint spots of the $(2x2)_C$ [32] reconstructions are also observed (see figure 5). Some samples have been annealed for a long time (typically 2 hours) at 950°C-1000°C (i. e. below the graphitization temperature) to promote the transformation of the SiC surface reconstruction from (3x3) to $(2x2)_C$ following the observations of Ref. 32. Auger spectroscopy and STM images show that the average graphene coverage was less than one layer for all the samples studied. The STM experiments were performed under UHV conditions at room temperature using PtIr tips, with tunnelling current I in the range 0.2-1.0 nA. The tunnelling bias V is applied on the sample. The data have been processed using the WsXM software [33].

1.2. ab-initio calculations

Calculations are performed with the VASP code based on density functional theory and a plane wave basis [34]. The GGA functional is used in the Perdew and Wang formulation [35]. The ultrasoft pseudopotentials have been extensively tested [10, 36]. The slabs contain 4 SiC bilayers and the dangling bonds on the opposite Si face are saturated with H atoms. Convergence is reached when forces are smaller than 0.01 eV/ Å. Integration in the Brillouin zone are performed with a 3x3x2 grid in the Monckhorst-Pack scheme.

2. The bare 6H-SiC(000-1) (3x3) surface

2.1. Scanning tunnelling microscopy and spectroscopy

The STM experiments reported in this section have been performed on bare substrate areas of lightly graphitized surfaces (see section 3 below). This insures that they have experienced the same thermal treatment as the graphene covered regions. A dual bias image of the same spot of the bare SiC(3x3) is shown in figure 1-a. The characteristic features of the SiC(3x3) reconstruction already reported by Hoster et al. [31] show up in this figure, and we adopt their notation to identify the remarkable sites A, B and C. Sites A and B appear equivalent (within a 180° rotation) in occupied state images but not in the empty state images [31]. Notice also that the C sites appear lower than the A and B sites at both polarities, which mean that they are presumably located below the highest surface plane.

A careful examination of a larger scale image (figure 1-b) reveals that all the C sites are not equivalent: some appear darker (lower) than the others. This difference shows up more clearly on the profile taken on the blue (grey) line in figure 1-b and depicted in figure 1-c: one can see "shallow" C sites with depth ≈0.9 Å and "deep" C sites with depth ≈1.2 Å. To our knowledge, this differentiation of the C sites has not been quoted before [31], although it has a strong impact on the surface electronic structure as shown below.

We have performed scanning tunnelling spectroscopy (STS) on the various sites of the SiC(3x3) reconstruction. For that purpose, I(V) spectra were recorded for all the points of a constant current image (the so-called CITS mode [37]). After numerical differentiation of the spectra, one can extract from this data set either site resolved dI/dV spectra or conductance maps at selected biases. A typical result is shown in figure 2. Figure 2-a is the constant current image, were one identifies the characteristic features of the SiC(3x3) reconstruction, including the "shallow" and "deep" C sites (the A and B sites were identified from a separate dual bias image as in figure 1-a and 1-b). Site resolved dI/dV spectra are shown in figure 2-b. All the spectra share common characteristics: a large increase in the conductance below -1.4 eV and just above the Fermi level, with a peak located around +0.7 eV, and a drastic reduction of the conductance in between (from -1.4 to +0.1 eV). These features are consistent with the average spectrum of the SiC(3x3) reported in [30], and they indicate the presence of a wide surface gap extending just below the Fermi level for the SiC(3x3) surface. In the occupied states, the conductance rise at about -1.5 eV is consistent with the onset of a strong photoemission signal in this range reported in a previous experiment [12]. However one notices a significant difference between the sites. On the A, B and some of the C sites -denoted as C- sites- the conductance (and the current, not shown) is actually very small between +0.1 V and -1.4 V, as expected for a surface gap. Conversely, a weak but non zero conductance is measured on the remaining C sites -denoted as C+ sites- in this energy range (except in a small interval close to zero bias, about 0.25 eV wide). There as thus "in gap" states located on the C+ sites (a faint feature similar to these "in gap" states also seems to be present in the photoemission data [12]). A conductance image recorded at the bias corresponding to the maximum of the conductance on the C+ sites (-0.67 eV) is shown in figure 2-c. From the comparison with the "topographic" image in figure 2-a, it appears that the C+ sites

correspond to the “shallow” C sites in constant current images (a light grid is overlaid on the images for comparison). From measurements on different images, the C+ (“shallow”) sites represent between 60% and 70% of the total number of C sites. Assuming, from spectroscopic data (figure 2-b) that each C+ site supports an “in gap” state and that these states are distributed in a 1 eV energy range (the typical surface gap size), this corresponds to a density of states per unit area (DOS) in the gap of the order of 8-10 10^{13} $eV^{-1}.cm^{-2}$. This is a quite sizeable value, large enough to pin the Fermi level at the surface of the SiC(3x3) reconstruction at the top of the gap for moderate doping levels of the substrate [38]. This large “in-gap” DOS may also hamper the control of the charge of a graphene overlayer by an external gate if strong hole doping has to be achieved. Indeed, the DOS on the C+ sites is comparable with the graphene DOS (which amounts to ≈6 10^{13} $eV^{-1}.cm^{-2}$ at 0.5 eV from the Dirac point [5]). The “shallow” (C+) sites are thus important for controlling the position of the Fermi level at the SiC(3x3) surface. However, since the C sites are located in subsurface positions as quoted above, the “in gap” states should couple only weakly with the graphene states of the overlayer [30].

2.2. “ab-initio” calculations

Although the (3x3) reconstruction has been known for decades, no atomistic model satisfactorily describes it. We investigated different configurations either from the literature (Hoster's et al [31]) or from well known semiconductor surface reconstructions (DAS model [39]). A simple bulk truncated structure (in 1x1 and 3x3 supercells) and a 3x3 cell with adatoms (3 Si adatoms) have also been calculated to search for clues for the reconstruction geometry. They are briefly described in the following. All these configurations can be ruled out in view of the STM images and more complex reconstruction mechanisms have to be searched for.

In agreement with Sabbisch et al [40] relaxation of the bulk-truncated geometry results in a strong inward shift toward the bulk of the surface bilayer together with a flattening of this bilayer (bilayer corrugation 0.35 Å instead of 0.61 Å in the bulk). The inter-bilayer distance is slightly increased (2 Å instead of 1.91 Å). The C dangling bonds give rise to a peak in the DOS located at the Fermi level. This peak is sharp for calculations performed in a 1x1 cell and tends to split into two components in a 3x3 supercell. This splitting goes with a buckling of the surface first plane in the 3x3 cell (corrugation 0.2 Å) and forces are difficult to minimize in the subsurface Si layer. Si adatoms (3 atoms per 3x3 cell) prefer H3 positions (Total energies : H3 : -577.19917 eV, T4 : -576.84598 eV, Top : not stable). This is surprising since in tetrahedral (Si, Ge) semiconductors, adatoms on the (111) surface go to T4 sites that are four fold coordinated [41] but it is coherent with what is found for the $(2x2)_C$ reconstruction. From these calculations, we can deduce that the surprising H3 site has to be considered for adatoms in the search of a possible 3x3 geometry and that a surface bilayer will be fractional as proposed in the literature [31].

The DAS model describes the famous (7x7) reconstruction of the Si (111) surface. The (9x9) and (5x5) reconstructions have also been observed on the same surface and can be described within

this model. The reconstruction (Fig 3-a) consists in two bilayers plus adatoms lying over the bulk crystal (represented by three additional bilayers in the calculation). The stacking of one half of the cell is faulted. This model can be adapted to a 3x3 periodicity. In this case it only involves two adatoms. Keeping in mind the mechanisms involved in the $SiC(2x2)_C$ reconstruction [36], we chose to use one Si and one C adatom to induce charge transfer so that one half of the unit cell would appear in empty states and the other one in filled states as observed on the STM images of the 3x3 reconstruction. For the same reason the C restatom was put in the faulted part : on a Si(111) surface this part is more charged than the other one [41]. It was possible to relax the structure so that the residual forces are lower than 0.01 eV/Å. The corresponding density of states is shown in figure 3-b. Inserts give the partial charge integrated on the peak area pointed by the arrows. They show only a protrusion on the Si adatom for filled states and on the C adatom for empty states in contradiction with STM images, ruling out this model.

Hoster et al.'s model (Fig. 4) does not include any information about the chemical nature of the reconstruction atoms. In our study, we chose to build the reconstruction fractional bilayer starting from a SiC bilayer (hence in figure 4-a, numbers 1 to 7 label Si atoms and 8, 9 and 10 indicate C atoms). The structure showed important convergence problems, hence, we could not relax the structure. Nevertheless, it is interesting to analyse general trends in the movements of the atoms and how it allows to form or to break bonds. After hundreds of relaxation steps, bonds indeed form between the atoms (1, 8, 2), (3, 9, 4) and (6, 10, 5), see figure 4-a. The atom 7 forms bonds with 8, 9 and 10. The surface reconstruction is bonded to the bulk-truncated surface through the atoms 1 to 6. However, at variance with the model structure, the atom 7 does not bind to its C neighbor from the bulk. Importantly, bonds around C and B sites expected by Hoster et al. [31] are missing (namely between atoms (3, 6), (1, 4) and (5, 2)). This suggests that this geometrical arrangement is not compatible with the covalent radii for Si and C. Note that the bond between atoms 1 and 6 was present in the initial configuration but had to be broken in order to form the bonds between (1, 8) and (6, 10).

In summary, none of the proposed nor anticipated models could give a satisfactory account of the SiC(3x3) atomic structure. It has to be noticed that, from the present and previous reports [40], the behaviour of the bulk truncated or adatoms decorated SiC(000-1) surface is quite odd with respect to the one of usual semiconductors. Thus, more elaborate models, taking into account phenomena more complex than the usual dangling bond saturation and charge transfer mechanisms, should probably be looked for.

3. Graphene monolayer on the 6H-SiC(000-1) (3x3) surface

3.1. Structure and doping

A large scale image of the lightly graphitized surface is shown in figure 5-a. The morphology of the surface, typical of UHV grown samples [27, 28, 30], consists in small graphene islands (bright

areas) a few 10 nm's wide, separated by regions of bare SiC(3x3) (dark areas). The graphene islands, hereafter denoted G_3x3, are typically 2.3-3.0 Å higher than the bare SiC(3x3) surface (depending on the tip and bias). These values are consistent with a graphene monolayer (see section 3.2 for further discussion). The G_3x3 islands show different superstructures in the nanometre range. They are related to different orientations of the graphene layer with respect to the underlying SiC(3x3) surface and have been identified as moiré patterns [30].

Figures 5-b and 5-c show images of the same region taken close to the edge of a G_3x3 island (the edge is on the left of the images). On the high bias images (figure 5-b), the graphene is "transparent" [27, 28, 30, 42, 43] (this point will be further considered in section 3.2) and one clearly sees the underlying SiC(3x3) substrate reconstruction. At low bias, figure 5-c, the graphene signal dominates in the STM images [28, 30], which is expected since the SiC(3x3) DOS is quite weak close to the Fermi level (see figure 2-b). Far from the boundary, e.g. in the boxed area of figure 5-c, the atomic contrast of the graphene layer is of the honeycomb type. This atomic contrast reflects the weak electronic coupling of the graphene layer with the SiC(3x3) surface reconstruction reported previously [12, 27, 30]. Close to the boundary a superstructure develops at the atomic scale, as in the region labelled R3 in figure 5-c. It is commensurate with the graphene lattice, with a $\sqrt{3}x\sqrt{3}R(30°)$ (R3) periodicity revealed in Fourier transformed images (not shown). The observation of the R3 superstructure in low bias STM images is well documented for graphite [44, 45, 46, 47] and graphene [43, 48, 49, 50, 51, 52, 53, 54]: it appears in the vicinity of sharp defects (point defects, steps or islands edges) and it is due to quantum interference (QI) effects [43, 45, 48, 49, 50, 51, 52, 54, 55, 56] which arise due to the scattering of the electron waves by these defects [57, 58]. The R3 periodicity is due to the special shape of the Fermi surface of graphene, which consists of small pockets (for doped samples) in the vicinity of the K/K' points of the surface Brillouin zone (sBZ), and it is related to "intervalley" scattering events [43, 45, 48, 49, 51, 52, 55, 56]. The absence of sublattice asymmetry in images taken far from the island edge, together with the observation of this R3 superstructure, indicates that the low energy electronic structure of G_3x3 is similar to the one of graphene (or graphite) [27, 30].

As for other 2D electron gases, it has been shown that the Fourier transform of the QI patterns which develop in the vicinity of defects in low bias STM images of graphene could provide a picture of the Fermi surface, and thus an indication of the doping level, of the sample [48, 49, 52, 54, 55, 56]. Our analysis shows that the doping level of graphene in G_3x3 islands is definitely smaller than for graphene monolayer on the Si face [48, 49, 52, 54] (the analysis was performed in the same conditions as in [52, 54] for the Si face, thus the difference is not related to room temperature conditions). We estimate a value of the Fermi wavevector $q_F=0.032\pm0.010$ Å^{-1} for G_3x3 (for comparison, $q_F\approx0.06$ Å^{-1} for graphene on the Si face [48, 49, 54]). Although this method does not give the sign of the doping, this value of q_F is consistent with a Dirac point located around 200 meV below the Fermi level, as reported in an photoemission study of submonolayer graphene films grown in UHV on the SiC-C face

[12]. It would corresponds to a carrier density in the few 10^{12} cm^{-2} range, which is the typical value obtained from transport measurements on multilayer samples grown by the CCS technique [4, 20], although in this latter case the interface structure is unknown.

3.2. "Transparency" of the graphene layer at high bias

By taking high bias images at a boundary between a G_3x3 island and the bare SiC(3x3) surface we can image with the same tip the electronic states of the (3x3) reconstruction with or without a graphene overlayer. This allows getting quantitative information on the "transparency" of graphene quoted in the previous section. The procedure is illustrated in figure 6. In figure 6-a the boundary is shown. The height of the G_3x3 island with respect to the bare (3x3) surface is h=2.72 Å. Zoomed-in images on the bare SiC(3x3) surface and on the G_3x3 island are displayed in figures 6-b and 6-c respectively. A faint graphene signal is observed on the G_3x3 island. We have taken profiles on the constant current images along the lines drawn in figures 6-b and 6-c. The profiles are compared in figure 6-d: the corrugation of the SiC(3x3) reconstruction is reduced only by a factor of 5 (typically) on the G_3x3 islands. Current-separation (I(s)) curves taken on the bare SiC(3x3) surface at the same bias (-2.5 V) show that the current decreases by a factor of 6 (typically, slightly site dependent) for a 1.0 Å increase in the tip-sample separation s (the I(s) curves, not shown, are exponential for Δs=1.0 Å). Extrapolating this value to the vertical position of the tip on the G_3x3 island -which is h=2.72 Å higher- would imply that the current coming from the (3x3) surface is reduced by a factor $(6)^{2.72}$=126 if the attenuation length of the (3x3) surface electronic states is assumed to be the same for the bare and graphene covered surface. Thus the contribution of the SiC(3x3) states to the total current would be of the order of 1%, which means that one would hardly identify any (3x3) related structures on G_3x3 islands. Specifically, this is clearly inconsistent with the measured (3x3) corrugations shown in figure 6-d. In terms of its order of magnitude, similar results have been obtained on different G_3x3/bare SiC(3x3) boundaries from different samples and using different tips. Our conclusion is that a mechanism should enhance the evanescent part of the SiC(3x3) occupied surface states wavefunctions -so that the corresponding LDOS is shifted away from the surface in the vacuum region- when it is capped by a graphene layer.

This conclusion can be extended to a larger energy range by examining tunnelling spectra taken either on the bare SiC(3x3) surface or on the G_3x3 islands of figure 6-a and shown in figure 6-e (these are average spectra taken on defect-free zones, extracted from a CITS experiment). The characteristic features of the bare SiC(3x3) surface show up in the corresponding spectrum (red/gray dashed curve): a large increase in conductance below -1.4 V and a broad peak centered just below +1.0 V. As previously reported [30], the same features are also apparent in the spectra recorded on the G_3x3 island (blue/dark plain curve). Their amplitude is only reduced by a factor of ≈2 for the conductance jump at -1.4 V and 5-6 for the +1.0V peak. The same argument as before, using the measured values of the current decay length and island height at the stabilisation voltage of the spectra

(-2.5V) for this CITS experiment, again shows that the contribution of the SiC(3x3) states to the tunnelling current on the G_3x3 islands should be only of the order of 1% without an amplification of the evanescent part of those states in vacuum. The tunnelling spectra suggest that such amplification should occur, not only at large negative bias but also at moderate positive bias. Indeed, the data of Ref. 30 show that the SiC(3x3) states dominate the STM images of the G_3x3 islands at +0.5 and +1.0 V. Notice that a similar behaviour has been reported in the literature for insulating layers on metallic surfaces. For example, a Xe monolayer (or NaCl double layer) on Cu(111) appears transparent in STM images, allowing to probe the Cu Shockley surface state through the insulating layer [59, 60]. Moreover, it has been stated in Ref. 59 that the Cu surface state shows a smaller decay rate through a Xe monolayer than trough vacuum.

The high bias transparency of graphene on the SiC-Si face has been ascribed in previous reports to a larger DOS of the substrate compared to that of graphene [42, 43] or to a small extension in vacuum of the graphene states which forces the tip to come close to the substrate [43, 61]. Both effects play a role, but in addition our analysis indicates that the enhancement of the evanescent part of the electronic states of the SiC(3x3) surface by the graphene layer also has an important effect. It increases the LDOS of the SiC surface states in vacuum so that it becomes of the order of, or larger than, the small and rapidly [62] decaying LDOS of graphene at a larger distance from the substrate (compared to the bare SiC surface). This enhancement is probably due to the modification by the graphene layer of the potential felt outside the SiC crystal by the electrons of the SiC(3x3) states. We consider that, owing to the weak graphene-SiC(3x3) interaction [30], only the evanescent part of the SiC(3x3) surface states is affected by the graphene overlayer (i.e. that the DOS of those states remains almost unaffected in the SiC surface plane). We can thus model the enhancement effect of the graphene layer in a rough way, by simply treating this carbon plane as a potential well of width d and depth V which reduces the potential outside the SiC surface (V=0 means no graphene, d has been fixed to 3.3 Å which is the interlayer distance in graphite). A similar model has been applied to describe STM imaging of insulator-metal interfaces [63]. A picture of the potential profile seen outside the substrate by an electron in an SiC(3x3) surface state (thick horizontal bar) is depicted in the inset of figure 6-f. We solve a one dimensional Schrödinger equation for k//=0 [64] outside the SiC substrate with the constrain of a constant amplitude for the SiC surface state in the substrate surface plane (the x=0 plane). As expected, when V increases, the point where the evanescent part of the SiC(3x3) surface state has a given modulus shifts away from the substrate surface. We plot in figure 6-f this shift Δx as a function of V for a state located 6 eV below the vacuum level, this is 1.5-2 eV below the Fermi level. Away from the resonance at V≈8 eV, which is irrelevant in view of the crudeness of the model, we get values of Δx of the order of a couple of Å's. The model is thus globally consistent with the data of figure 6-b to 6-e, which suggests that the contribution of the total tunnelling current arising from the SiC(3x3) surface is reduced by a factor 2 to 5 for a tip height variation of 2.7 Å. The model we propose is indeed highly simplified, including neither the image term of the external

potential [60, 66, 67] nor the band structure and electron states of graphene, which shows a gap extending from -3eV to +3eV at k//=0 [68]. It can thus only give the order of magnitude of the "transparency" effect.

4. Stability of the interface reconstruction

We now examine the thermal stability of the SiC(3x3) reconstruction. Figure 7-a shows the LEED pattern of a sample covered with ≈ 1 ML graphene just after the graphitization stage (see section 1). The most intense diffraction spots of the SiC substrate surface are those of the (3x3) reconstruction (yellow/light gray arrows), although faint spots of the $(2x2)_C$ reconstruction are also visible (blue/grey squares). The STM image of figure 5-a has been obtained on this sample. Images taken at various spots of the surface reveal a mixture of G_2x2 and G_3x3 islands [27], but the bare substrate surface only shows the SiC(3x3) reconstruction (G_2x2 denotes a monolayer graphene island on top of the $SiC(2x2)_C$ substrate reconstruction). Upon subsequent long annealing below the graphitization temperature (in that case: 80 minutes at 950-1000°C), the spots of the $SiC(2x2)_C$ reconstruction become more intense than those of the (3x3) in the LEED pattern (figure 7-b). The graphene signal remains unchanged. This transformation of the SiC(3x3) reconstruction into the $SiC(2x2)_C$ one after extensive annealing has been reported previously in a LEED investigation by Bernhardt et al. [32] and we have basically followed their recipe. When the transformed sample is examined by STM, we notice that extended and well ordered areas of the $SiC(2x2)_C$ reconstruction are only located *below* a graphene layer (i. e. in G_2x2 islands). The bare substrate surface itself remains (3x3) reconstructed, except for very small patches (less than 10 nm in size) of $(2x2)_C$ reconstructions. This is illustrated in figure 7-c to 7-e, for STM images of the sample corresponding to the LEED pattern in figure 7-b. In figure 7-c, one can see large G_2x2 islands (bottom, bright). The bare substrate surface (top, dark) mostly exhibits the (3x3) reconstruction, except at some spots located close to the G_2x2 islands (for instance in the box labelled II in figure 7-c) where a $(2x2)_C$ structure shows up. Zoomed in images on $SiC(2x2)_C$ areas of the bare substrate (figure 7-e) show that they form small patches with high disorder. Conversely, the $SiC(2x2)_C$ reconstruction forms extended (a few 10 nm's) and well ordered regions in the G_2x2 islands (figure 7-d). The same observation of a selective (3x3) to $(2x2)_C$ transformation can be made in partially transformed samples such as the one shown in figure 7-f (taken from another sample). Areas labelled A (B) are G_3x3 (G_2x2) islands respectively. In this region most of the islands are G_2x2. However, zoomed in images on the bare substrate surface (dark areas) show the (3x3) reconstruction everywhere, without any patch of $(2x2)_C$ (on this high definition image atomic resolution is well defined in numerically zoomed-in images). The black arrows in figure 7-f indicate boundaries between G_2x2 and G_3x3 phases within the same island. We ascribe these boundaries to an incomplete transformation of the SiC(3x3) into $SiC(2x2)_C$ below the graphene layer. We have observed a number of such composite islands. Atomic resolution images (not shown) demonstrate that the graphene layer has the same orientation and that the atomic rows are

aligned on both phases. This suggests that the graphene plane is continuous over the G_3x3/G_2x2 boundary of mixed islands, as expected for an island whose transformation has been blocked when the annealing was stopped.

These experiments show that a transformation of the substrate surface reconstruction from SiC(3x3) into $SiC(2x2)_C$ takes place below the graphene layer, at least at low temperatures. It is however rather slow, as noticed previously [32], and does not seem to proceed much faster at higher temperatures. Indeed, LEED patterns taken on more heavily graphitized samples (average number of planes from 2 to 4.5), prepared by annealing for 10-30 minutes at temperatures higher by 100-150°C than the onset of graphitization, still show a dominant SiC(3x3) reconstruction at the interface. Together with the fact that G_2x2 islands are often detected right after graphitization in lightly graphitized samples, these observations suggest that it may be difficult to obtain a *totally* homogeneous reconstruction at the graphene-SiC interface for the C face. It is however possible to get an *almost* pure SiC(3x3) reconstruction at the interface without extensive annealing.

One puzzling observation is that the evolution from SiC(3x3) to $SiC(2x2)_C$ is more efficient below the graphene layer than on the free surface in our experimental conditions. In a previous report we have shown evidences for a larger interaction of the graphene layer with the $SiC(2x2)_C$ reconstruction than with the SiC(3x3) surface [27]. We believe that this larger interaction provides an additional driving force which results in an easier transformation of the graphene covered surface from SiC(3x3) to $SiC(2x2)_C$. Of course one should also consider that the two SiC surface reconstructions do not have the same atomic density and/or composition [32]. Hence the (3x3) to $(2x2)_C$ transformation involves either some long range diffusion or the evaporation of adatoms. A graphene overlayer should not favour evaporation [69]. Nevertheless, the structural homogeneity of the G_2x2 islands indicates that the difference in adatom density is efficiently managed in graphene covered areas during the transformation (on the scale of our islands sizes, which are typically 10 nm's wide. It may be different for much larger islands).

We have identified the slow structural transformation of the substrate surface reconstruction as a source of interfacial heterogeneity. It turns out that the density of a common kind of defects of the G_2x2 phase [70] varies significantly from one G_2x2 island to the other (although their density remains in the 10^{12} cm^{-2} range, data not shown). Since we have found that these specific defects were able to transfer charge to the graphene layer [70, 71], this should result in a different doping level of neighbouring G_2x2 islands. There is thus heterogeneity of electronic origin at the interface in our samples, in addition to the structural one.

5. Summary and conclusions

We have presented a detailed characterization at the atomic scale of the interface between graphene and the 6H-SiC(000-1) substrate. The objective was to understand the mechanisms which can lead to local variations in the chemical and electronic structure of the interface. By analyzing

classical models by ab initio calculations we show that the SiC(3x3) reconstruction should have an unusual structure. Experimentally, this reconstruction shows a significant density of in-gap states. These states are on subsurface sites, and thus should not interact significantly with the graphene states. Moreover they do not induce a strong layer doping. It is also shown that the graphene layer enhances the evanescent part of the wavefunctions of the SiC(3x3) electron states, which contributes to the high-bias transparency of graphene. Finally, we investigate the thermal stability of the SiC(3x3) reconstruction. It is shown to evolve slowly into a $SiC(2x2)_C$. This transformation takes place more easily below the graphene layer than for the bare surface. We believe that this selectivity is related to a stronger interaction of the graphene layer with the $SiC(2x2)_C$. This slow transformation, together with the local variations of the defect density on the $SiC(2x2)_C$ reconstruction, lead to an heterogeneous interface for our UHV grown samples.

Acknowledgments

This work was supported by the French ANR ("GraphSiC" Project No. ANR-07-BLAN-0161), by the Région Rhône-Alpes ("Cible07", "Cible08" and "Cluster micro-nano" programs) and by the "Fondation Nanosciences" (project RTRA "DispoGraph"). F.H. held a doctoral support from la Région Rhône-Alpes. We thank A. Mahmood for valuable collaboration.

References

[1] Novoselov K S, Geim A K, Morozov S V, Jiang D, Katsnelson M I, Grigorieva I V, Dubonos A A and Firsov A A 2005 *Nature* **438** 197

[2] Zhang Y, Tan Y-W, Stormer H L and Kim P 2005 *Nature* **438** 201

[3] Berger C *et al* 2004 *J. Phys. Chem.* B **108** 19912

[4] Berger C *et al* 2006 *Science* **312** 1191

[5] Ohta T, Bostwick A, McChesney J L, Seyller T, Horn K and Rotenberg E 2007 *Phys. Rev. Lett.* **98** 206802

[6] Zhou S Y, Gweon G H, Fedorov A V, First P N, de Heer W A, Lee D-H, Guinea F, Castro Neto A H and Lanzara A 2007 *Nature Materials* **6** 770

[7] Adam S, Hwang H E, Rossi E and Das Sarma S 2009 *Solid. State Comm.* **149** 1072

[8] Tedesco J L et al. 2009 *Appl. Phys. Lett.* **95** 122102

[9] Varchon F *et al* 2007 *Phys. Rev. Lett.* **99** 126805

[10] Varchon F, Mallet P, Veuillen J-Y and Magaud L 2008 *Phys. Rev. B* **77** 235412

[11] Kim S, Ihm J, Choi H J and Son Y-W 2008 *Phys. Rev. Lett.* **100** 176802

[12] Emtsev K V, Speck F, Seyller T, Ley L and Riley J D 2008 *Phys. Rev.* B **77** 155303

[13] van Bommel A J, Crombeen J E and van Tooren A 1975 *Surf. Sci.* **48** 463

[14] Veuillen J Y, Hiebel F, Magaud L, Mallet P and varchon F 2010 *J. Phys. D: Appl. Phys.* **43** 374008

Ferrer F J, Moreau E, Vignaud D, Deresmes D, Godey S and Wallart X 2011 *J. Appl. Phys.* **109** 054307

[15] Emtsev K V *et al* 2009 *Nature Mater.* **8** 203

[16] Virojanadara C, Syväjarvi M, Yakimova R, Johansson L I, Zakharov A A and Balasubramanian T 2008 Phys. Rev. B **78**, 245403

[17] Tromp R M and Hannon J B 2009 *Phys. Rev. Lett.* **102** 106104

[18] Camara N, Huntzinger J-R, Rius G, Tiberj A, Mestres N, Pérez-Murano F, Godignon P and Camassel J 2009 *Phys. Rev. B* **80** 125410

[19] de Heer W. A. et al. 2011 arXiv:1103.3552

Haas J, de Heer W A and Conrad E H 2008 *J. Phys.: Condens. Matter* **20** 323202

[20] de Heer W A et al. 2010 *J. Phys. D: Appl. Phys*. **43** 374007

[21] Forbeaux I, Themlin J-M and Debever J-M 1998 *Phys. Rev. B* **58** 16396

[22] Riedl C, Coletti C, Iwasaki T, Zakharov AA and Starke U 2009 *Phys. Rev. Lett.* **103** 246804

[23] Virojanadara C, Zakharov A A, Yakimova R and Johansson L I 2010 *Surf. Sci. Lett.* **604** L4

[24] Gierz I et al 2010 *Phys. Rev. B* **81** 235408

[25] Speck F et al 2011 arXiv:1103.3997

[26] Forbeaux I, Themlin J-M and Debever J-M 1999 *Surf. Sc*i. **442** 9

[27] Hiebel F, Mallet P, Varchon F, Magaud L and Veuillen J-Y 2008 *Phys. Rev.* B **78** 153412

[28] Starke U and Riedl C 2009 *J. Phys.: Condens. Matter* **21** 134016

[29] Mathieu C, Barrett N, Rault J, Mi Y Y, Zhang B, de Heer W, Berger C, Conrad E H and Renault O 2011 *Phys. Rev. B* **83** 235436

[30] Hiebel F, Mallet P, Magaud L and Veuillen J-Y 2009 *Phys. Rev.* B **80** 235429

[31] Hoster H M, Kulakov M A and Bullemer B 1997 *Surf. Sci.* **382** L658

[32] Bernhardt J, Nerding M, Starke U and Heinz K 1999 *Materials Science and Engineering* **B61–62** 207

[33] Horcas I et al. 2007 *Rev. Sci. Instrum.* **78** 013705

[34] Kresse G and Hafner J 1993 *Phys. Rev. B* **47** 558

[35] Perdew J P and Wang Y 1986 *Phys. Rev. B* **33** 8800

[36] Magaud L, Hiebel F, Varchon F, Mallet P and Veuillen J-Y 2009 *Phys. Rev. B* **79** 161405(R)

[37] Hamers R J, Tromp R M and Demuth J E 1986 *Phys. Rev. Lett.* **56** 1972

[38] Lanno M and Friedel P 1991 *Atomic and Electronic Structure of Surfaces: Theoretical Foundations, Springer Series in Surface Science Vol. 16* (Heidelberg, Springer-Verlag)

[39] Takayanagi K et al. 1985 *Surf. Sci.* **164** 367

[40] Sabbisch M et al. 1997 *Phys. Rev. B* **55** 10561

[41] Stich I, Terakura K and Larson BE 1995 *Phys. Rev. Lett*. **74** 4491

[42] Rutter G M, Guisinger N P, Crain J N, Jarvis E A A, Stiles M D, Li T, First P N and Stroscio J A 2007 *Phys. Rev.* B **76** 235416

[43] Mallet P, Varchon F, Naud C, Magaud L, Berger C and Veuillen J-Y 2007 *Phys. Rev.* B **76** 041403(R)

[44] Mizes H A and Foster J S 1989 *Science* **244** 559

[45] Ruffieux P, Melle-Franco M, Gröning O, Bielmann M, Zerbetto F and Gröning P 2005 *Phys. Rev. B* **71** 153403

[46] Kobayashi Y, Fukui K, Enoki T, Kusakabe K and Kaburagi Y 2005 *Phys. Rev. B* **71** 193406

[47] Niimi Y, Matsui T, Kambara H, Tagami K, Tsukada M and Fukuyama H 2006 Phys. Rev. B **73** 085421

[48] Rutter G M, Crain J N, Guisinger N P, Li T, First P N and Stroscio J A 2007 *Science* **317**, 219

[49] Brihuega I *et al.* 2008 *Phys. Rev. Lett.* **101** 206802

[50] Rutter G M, Guisinger N P, Crain J N, First P N and Stroscio J A 2010 *Phys. Rev. B* **81** 245408

[51] Simon L, Bena C, Vonau F, Aubel D, Nasrallah H, Habar M and Peruchetti J C 2009 *Eur. Phys. J. B* **69** 351

[52] Yang H, Mayne A J, Boucherit M, Comtet G, Dujardin G and Kuk Y 2010 *Nano Lett.* **10** 943

[53] Ye M et al; 2010 *Eur. Phys. J. B* **75** 31

[54] Mahmood A, Mallet P and Veuillen J Y *to appear in Nanotechnology (in press)*

[55] Bena C 2008 *Phys. Rev. Lett.* **100** 076601

[56] Pereg-Barnea T and McDonald A H 2008 *Phys. Rev. B* **78** 014201

[57] Crommie M F, Lutz C P and Eigler D M 1993 *Nature (London)* **363** 524

[58] Hasegawa Y and Avouris P 1993 *Phys. Rev. Lett.* **71** 1071

[59] Park J-Y et al. 2000 *Phys. Rev. B* **62** 16341(R)

[60] Repp J, Meyer G and Rieder K-H 2004 *Phys. Rev. Lett.* **92** 036803

[61] Charrier A *et al* 2002 *J. Appl. Phys.* **92** 2479

[62] Zhang Y et al. 2008 *Nat. Phys.* **4** 627 suggest that the decay length of the graphene low energy states may however increase above the threshold for inelastic tunnelling.

[63] Sumetskii M I and Baranger H U 1995 *Appl. Phys. Lett.* **66** 1352

[64] k// is the momentum of the states // to the surface. The states with k//=0 have the smallest decay rate in vacuum [65]

[65] Wiesendanger R 1994 *Scanning Probe Microscopy and Spectroscopy* (Cambridge: Cambridge University Press))

[66] Silkin V M, Zhao J, Guinea F, Chulkov E V, Echenique P M and Petek H 2009 *Phys. Rev. B* **80** 121408(R)

[67] Bose S et al. 2010 *New J. Phys.* **12** 023028

[68] Latil S and Henrard L 2006 *Phys. Rev. Lett*. **97** 036803

[69] Camara N, Rius G, Huntzinger J-R, Tiberj A, Magaud L, Mestres N, Godignon P and Camassel J 2008 *Appl. Phys. Lett.* **93** 263102

[70] Hiebel F, Mallet P, Veuillen J-Y and Magaud L 2011 *Phys. Rev. B* **83** 075438

[71] Jayasekera T, Xu S, Kim K W and Nardelli M B 2011 *Phys. Rev. B* **8**4 035442

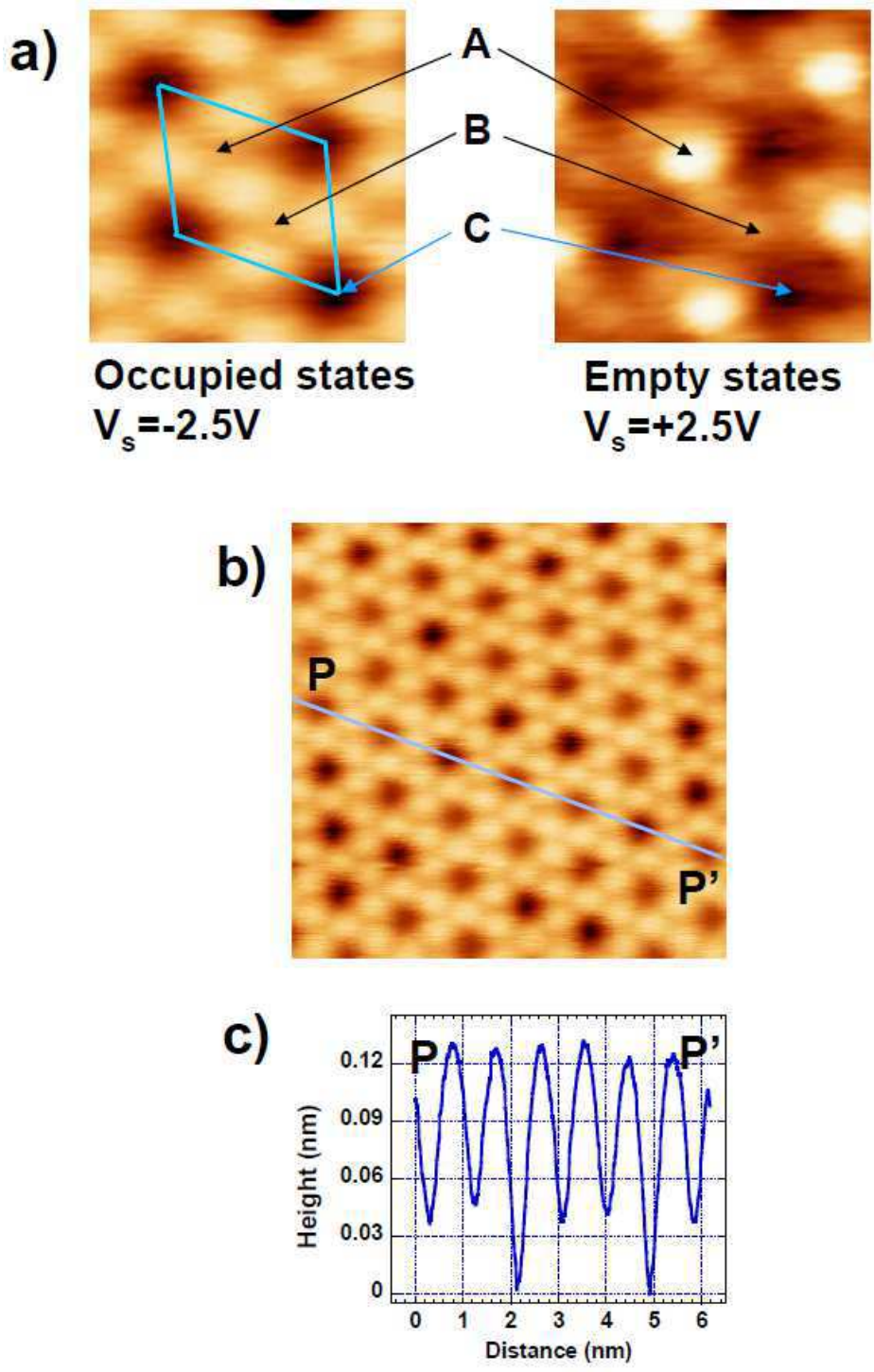

Figure 1: STM images of the bare SiC(3x3) surface. a) Dual bias image on the same area of the surface, image size: 1.7x1.8 nm². b) Occupied state image showing shallow and deep C sites. Image size: 5.8x5.8 nm², sample bias: -2.5V. c) Profile along the PP' line in b).

Figure 1

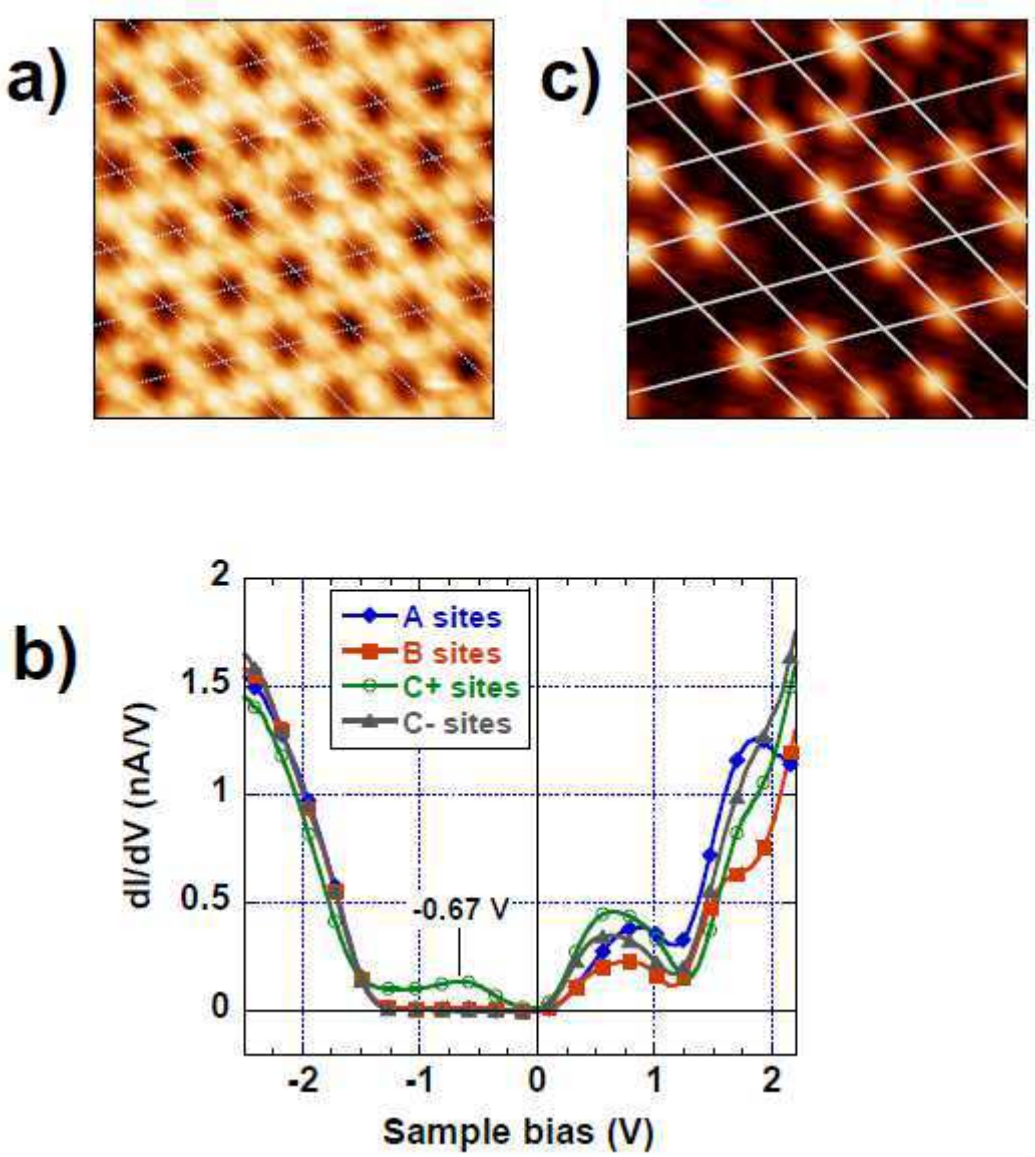

Figure 2: Tunnelling spectroscopy on the bare SiC(3x3) surface. a) Constant current image, size: 5.0x5.0 nm², sample bias: -2.5 V, tunnelling current 1.0 nA. b) Conductance (dI/dV) spectra taken on the different sites of the SiC(3x3) reconstruction (see figure 1). Each curve is an average over 10 equivalent sites in the image displayed in a). Stabilization conditions: bias -2.5 V, current: 1.0 nA. c) Conductance image at sample bias -0.67 V at the same spot as the image in a). A grid is overlaid on the images in a) and c) to help visualizing the location of the conductance features in the constant current image.

Figure 2

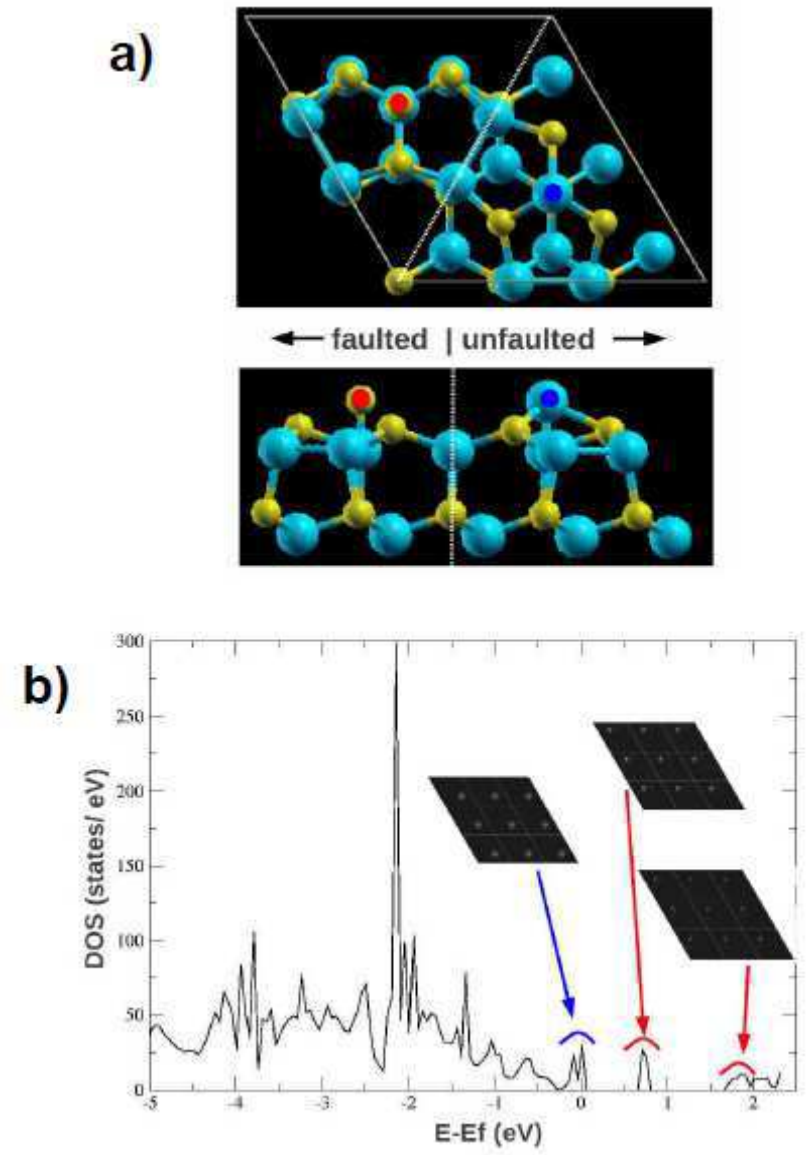

Figure 3: SiC(3x3) reconstruction in the DAS model. a) Relaxed configuration, top (up) and side(bottom) view. b) Computed density of states in this model. Inserts: modulus of the wavefunctions $|\Psi|^2$ integrated in the energy range of the peaks indicated by arrows. The colors (red and blue) refer to the C (red) and the Si (blue) adatoms

Figure 3

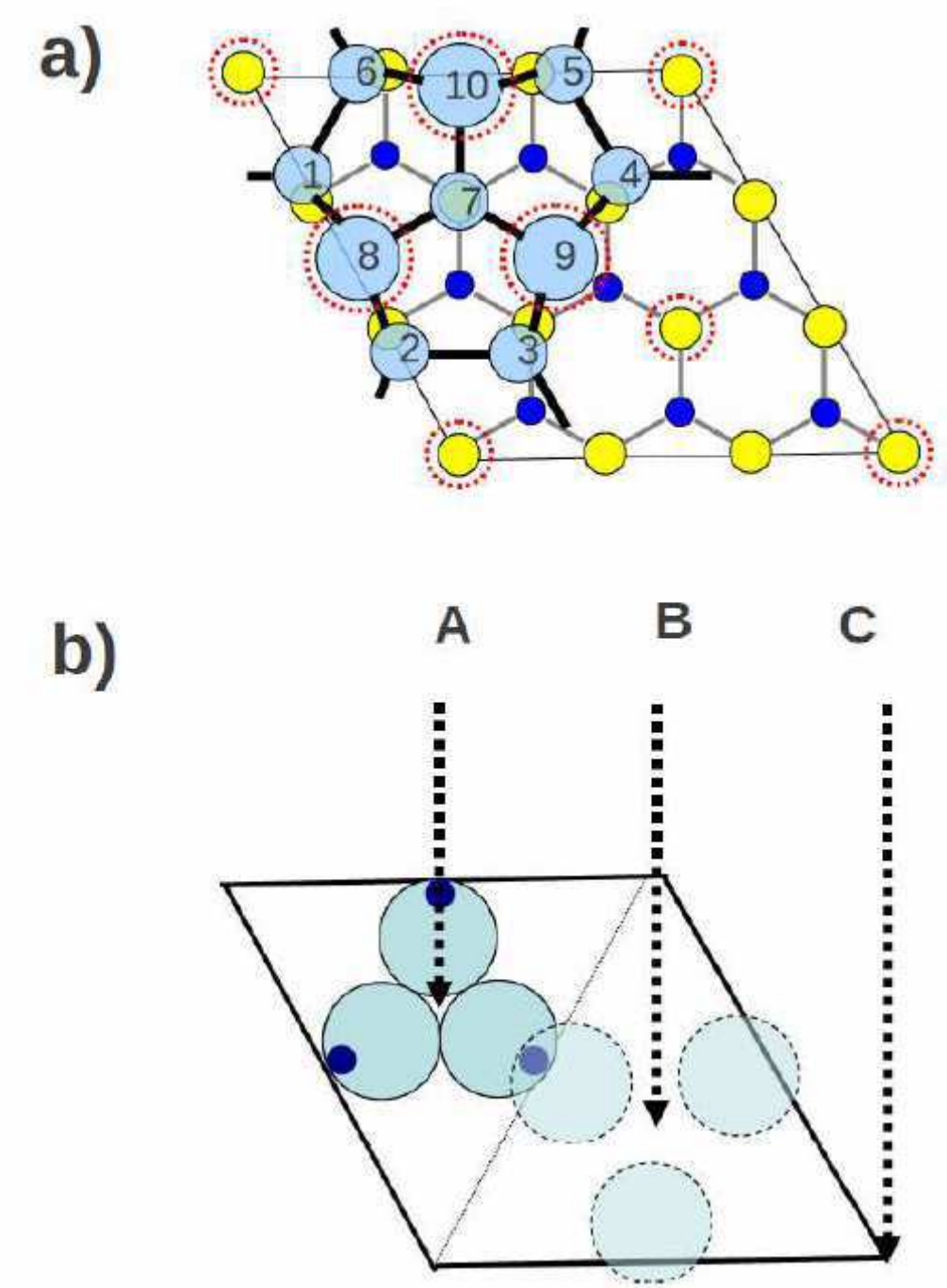

Figure 4: Hoster et al. 's model [31] of the SiC(3x3) surface reconstruction. (a) Geometrical arrangement: The last SiC bilayer is given in yellow (light grey) (C atoms) and blue (black) (Si atoms). The atoms that form the reconstruction are depicted in light blue (grey). Dangling bonds are indicated by dotted circles. The size of the atoms refers to their height. Larger atoms are higher.
(b) Hoster et al.'s interpretation of the STM images based on the dangling bonds belonging to the atoms 8, 9 and 10. The 3 atoms are represented by dots. Their orbitals are depicted by circles in solid line (empty orbitals) and dotted line (filled orbitals). The A, B and C sites (cf Fig. 1) are indicated by arrows.

Figure 4

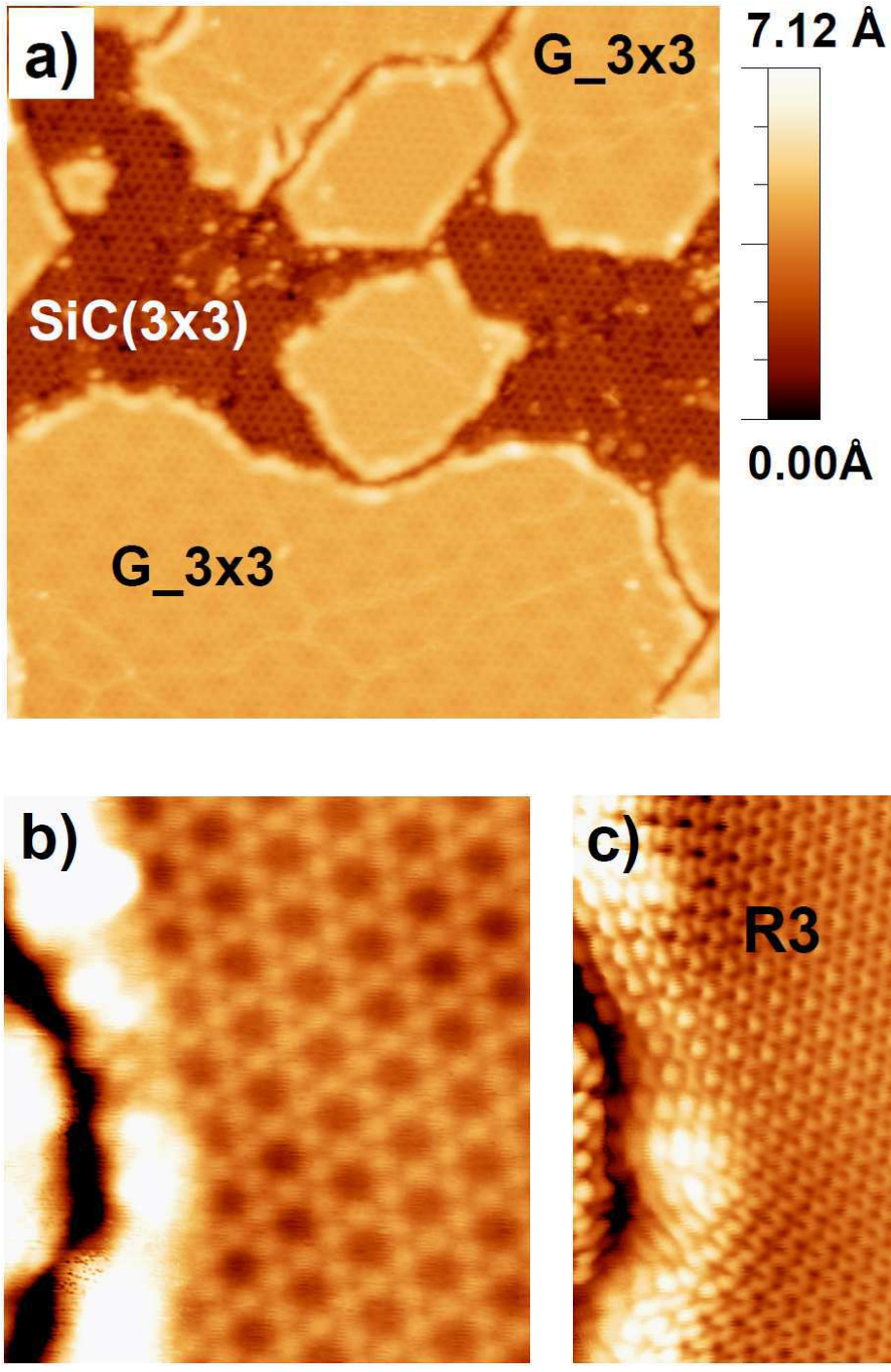

Figure 5: STM images of a sample just after graphitization. a) Overview. The dark areas are the bare SiC(3x3) surface. The light areas are G_3x3 islands (SiC(3x3) covered by 1 graphene layer). Image size: 50x50 nm², sample bias: -2.5 V. b) High bias image of a G_3x3 island. Sample bias: -2.5 V. The edge of the island shows up on the left side. c) Low bias image of the same region as in b). Sample bias: -100 mV. The honeycomb atomic contrast typical for graphene shows up within the island, for example in the boxed area. Closer to the island edge a $\sqrt{3}x\sqrt{3}R(30°)$ (R3) superstructure appears. Image size for b) and c): 6.4x6.9 nm².

Figure 5

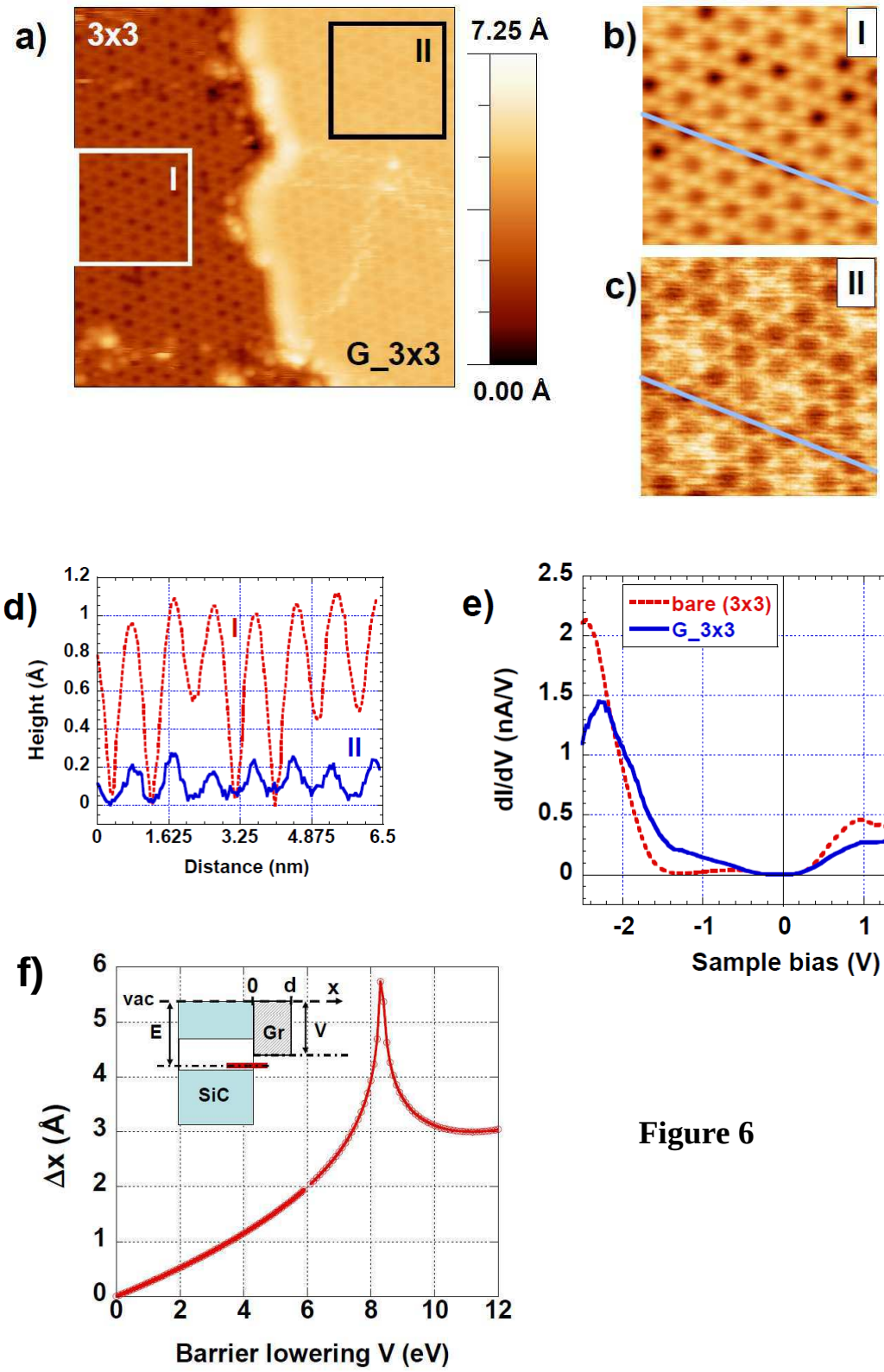

Figure 6

Figure 6: Transparency of graphene at high sample bias. a) High bias images (sample bias: -2.5 V) of a boundary between a G_3x3 island (right) and a bare SiC(3x3) surface (left). Image size: 20x20 nm². b) Zoomed-in image on the bare SiC(3x3) island in a) in the boxed area labelled I. Image size: 6x6 nm².c) Zoomed-in image on the G_3x3 island in a) in the boxed area labelled II. Image size: 6x6 nm². d) Profiles along the lines indicated in figures b) and c). Red dashed line: on the bare SiC(3x3) surface (zone I). Blue continuous line: on the G_3x3 island (zone II). e) Average conductance spectra on the

bare SiC(3x3) (red dashed line) and on the G_3x3 island (blue continuous line) in a). Stabilization conditions: sample bias: -2.5V, tunnelling current: 1.0 nA. f) Shift of the point where the modulus of the wavefunction of the SiC(3x3) surface state (thick red bar in the insert) has a given value when a potential well of width d and depth V mimicking a graphene layer is added to the bare SiC(3x3) surface potential. Inset: schematics of the potential profile at the surface (assuming sharp interfaces). The bare SiC(3x3) surface plane is at x=0.

Figure 6 continued

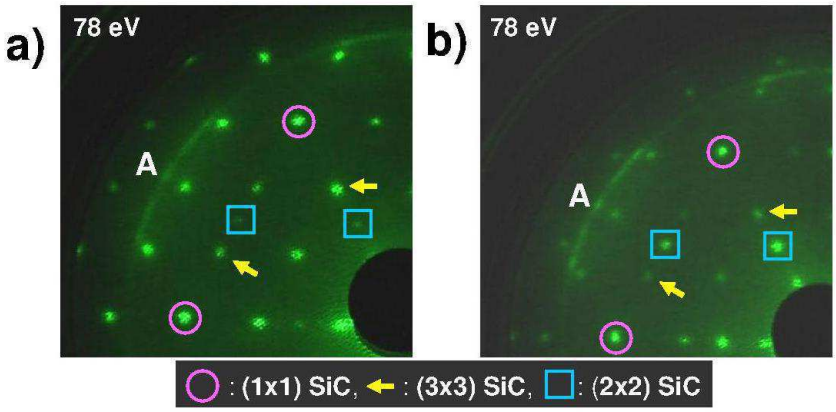
a)
78 eV
A
b)
78 eV
A
: (1x1) SiC, : (3x3) SiC, : (2x2) SiC

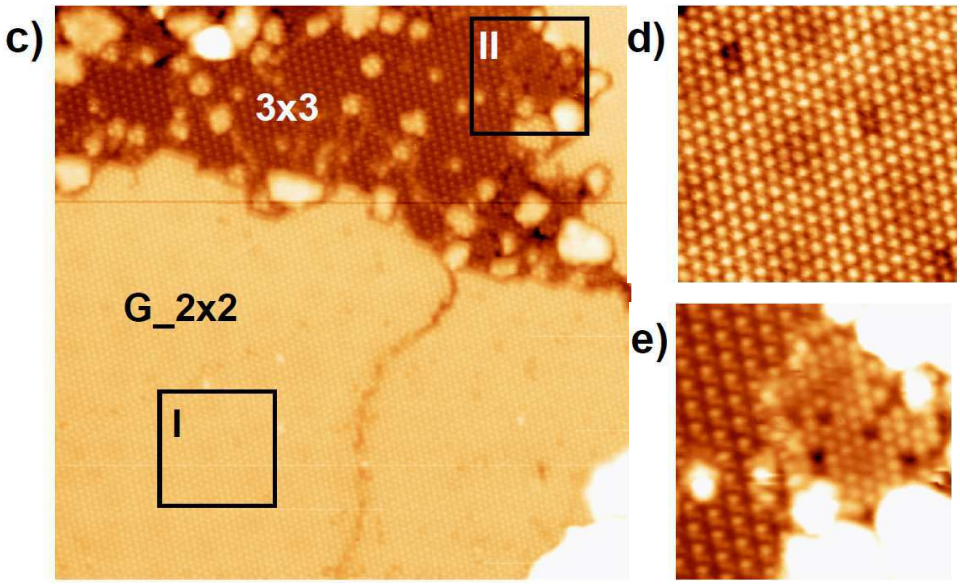
c)
II
3x3
G_2x2
I
d)
e)

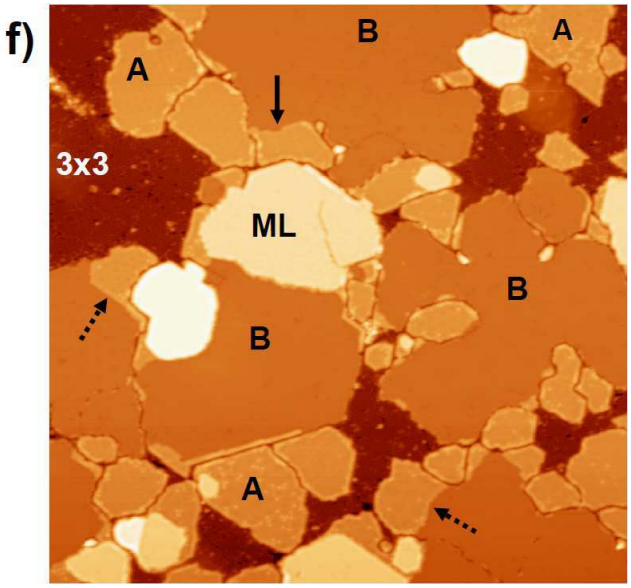
f)
A
B
A
3x3
ML
B
B
A

Figure 7

Figure 7: Transformation of the SiC(3x3) surface reconstruction upon annealing. a) LEED pattern of a freshly graphitized surface. b) LEED pattern of the same sample after 80 minutes annealing at 950-1000° C (below the graphitization temperature). For a) and b) the graphene signal is the arc (labelled A) and the diffraction spots of the SiC surface are indicated by circles, arrows and squares as shown below the figures. c) Image of the sample after the extended annealing (LEED pattern shown in b)). Image size: 50x50 nm², sample bias: +2.5 V. The bright area (bottom) is a G_2x2 island. The dark area (top) is the bare SiC surface, mostly (3x3) reconstructed. d) Zoomed-in image on the G_2x2 island in the boxed area labelled I in d). e) Zoomed-in image on the bare SiC surface in the area labelled II in d). A small zone showing a $(2x2)_C$ reconstruction shows up at the centre-right of the image. The left side exhibits the SiC(3x3) reconstruction. f) STM image of a graphitized sample without extended annealing. Only short annealing pulses at 950-1000° C (total duration 30') have been applied to clean the sample. Image size: 150x150 nm². The dark areas are the bare SiC(3x3) surface (no $SiC(2x2)_C$ is observed there). The areas labelled A (B) are G_3x3 (G_2x2) phases respectively. Arrows indicate boundaries between G_3x3 and G_2x2 zones within the same island.

Figure 7 continued